Maciej Boguń

Department of Man-Made Fibres
Faculty of Material Technologies
and Textile Design
Technical University of Lodz
ul. Żeromskiego 116, 90-924 Lodz, Poland
e-mail: maciek.bogun@wp.pl

Nanocomposite Calcium Alginate Fibres Containing SiO_2 and Bioglass

Abstract
An investigation was made of the effect of the basic parameters of the process of production of nanocomposite calcium alginate fibres containing silica and bioglass as nanoadditives. An analysis was made of the rheological properties of solutions, as well as of the porous and supramolecular structure and sorptive and strength properties of the fibres. The nanocomposite fibres obtained, depending on the as-spun draw ratio, achieved a tenacity of 19 – 22 cN/tex (in the case of nanosilica) and 16 – 24 cN/tex (in the case of bioglass). Both types of fibre have high sorptive properties and a high water retention value.

Key words: *nanocomposite, calcium alginate fibre, bioglass, nanoadditives.*

Introduction

Tissue engineering is one of the fastest-developing fields of medicine. Its purpose is to design and construct materials to be used in the regeneration of damaged tissue, such as bone tissue [1]. Available literature on the subject includes many papers concerning the production of various types of scaffolds. Among the main applications of tissue engineering, one can mention works that concern obtaining polymer and ceramic scaffolds aimed at regenerating the nervous system [2], skin [3], the liver [4], pancreas [5], bones [6] and the articular cartilage [7]. Currently on the market there are products for skin regeneration: ApliGraf and Dermagratf [8, 9] and for curing articular cartilage Bioseed [10].

Of increasing importance among that group of materials are scaffolds produced using various types of composites. The use of two groups of biocompatible materials, e.g. a resorbable polymer and another bioactive material, makes it possible to obtain a practically 'ideal' biocomposite for the regeneration of damaged tissue.

Consequently the concept was put forward of obtaining a scaffold on the basis of nanocomposite fibres made from calcium alginate (containing a SiO_2 or bioglass nanoadditive distributed in the material) and another resorbable polymer, such as polycaprolactone (PCL) or polilactide (PLA). In the literature of the subject works concerning polymer-fibrous composites on the basis of other polymers are present [11].

The nanoadditives are introduced into the fibres in order to give them osteoproductive properties. It is known, after all, that various types of bioactive glass and glass-ceramic composites are of great importance in implantology today. This is due to the particular role played by Si^{4+} in the creation of bone structures, as well as in the process of their calcification and regeneration following fractures [12]. At the present time, glass and composites of this type are used in, for example, the treatment of bone defects of the hip, the area of the knee joint and the spine [13 - 18].

The formation of scaffolds on the basis of nanocomposite alginate fibres requires that they demonstrate, apart from the basic biological properties, a strength sufficient for working alongside increased porosity. Both of these indicators depend directly on the structure produced during the solidification and drawing processes. Furthermore, the formation of fibres by the method of wet forming from solution makes it possible to control the process parameters so as to obtain the properties intended. In turn, the introduction of these fibres to a PGLA or PCL polymer matrix makes it possible to obtain a biocomposite with anisotropic properties characteristic of natural tissue, and with "dual-range" porosity. This will firstly be a porosity deriving from nanocomposite fibres of the order of 4 to 5000 nm, and secondly the porosity of the composite, exceeding 100 μm, produced using a porogen. The second porosity range is appropriate for the settling and growth of cells on the scaffold. Meanwhile porous alginate fibres are necessary for easier penetration of systemic fluids into their structure and acceleration of their resorbability.

The purpose of the research described in this paper was to determine the effect of the pull-out value at the as-spun draw ratio and the associated deformation value at the drawing stage on the supramolecular structure, strength properties, porous structure and sorptive properties of fibres made from calcium alginate containing an SiO_2 or bioglass nanoadditive. Conditions were identified for the production of nanocomposite fibres made from calcium alginate (containing, as alternatives, SiO_2 or bioglass). These fibres are intended to be used to obtain new types of biocomposites for use in tissue engineering.

Materials and methods

Spinning solutions were prepared using sodium alginate from FMC Biopolimer (Norway), whose trade name is Protanal LF 10/60LS, with intrinsic viscosity η = 3.16 dL/g. This polymer is characterised by a predominance of blocks derived from mannuronic acid (up to

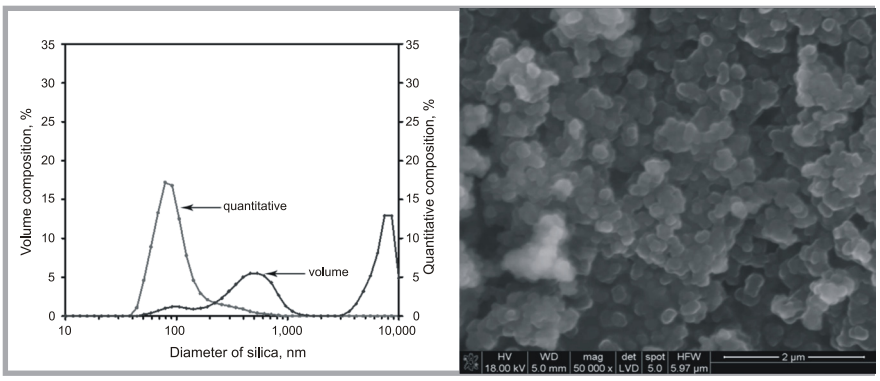

Figure 1. *Volume and quantitative composition and SEM photograph for SiO_2 nanoadditive.*

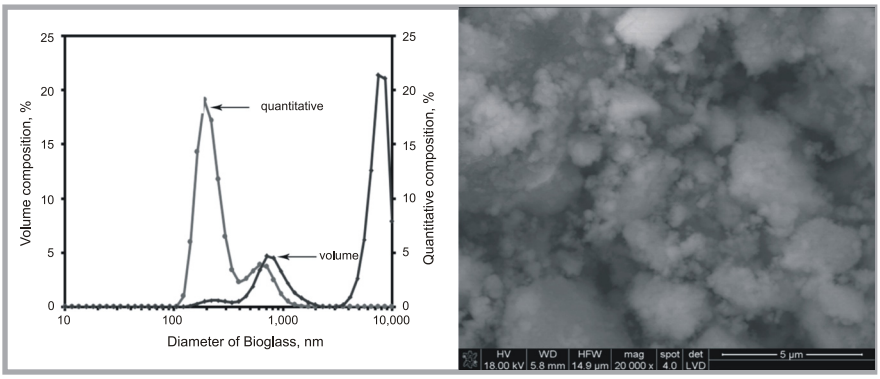

Figure 2. *Volume and quantitative composition and SEM photograph for bioglass nanoadditive.*

65%) over residues of guluronic acid. The nanoadditives used were nanosilica (Sigma Aldrich No. 637238) and bioglass obtained at Kraków University of Mining and Metallurgy (AGH). The nanoadditives were characterised at AGH, which involved measurement of the surface development by the gas adsorption method (BET), determination of particle size (DLS), and microscopic observation (SEM).

Measurements of the specific surface were performed with Nova 1200e apparatus from Quantachrome Inst., using the adsorption isotherm method (BET).

Particle sizes were investigated with Zetasizer Nano-ZS apparatus from Malvern Inc., using the technique of dynamic light scattering (DLS).

The nanosilica used has an average value of the specific surface of around 563.5 m^2/g, and average particle size of 60 – 100 nm (***Figure 1***). The bioglass used (oxide composition 16 %mol. CaO, 80 %mol. SiO_2, 4 %mol. P_2O_5) has an average specific surface value of around 220.2 m^2/g, and average particle size of 100–200 nm (***Figure 2***).

Fibre formation

Alginate fibres were formed by wet-spinning from solution using distilled water as the solvent. Based on the preliminary examinations, a concentration of sodium alginate in the water of 7.4% and a nanoadditive (SiO_2 or Bioglass) content of 3% in proportion to the polymer mass were selected.

Prior to being added to the spinning solution, the nanoadditive suspension was subjected to 30-minute ultrasound treatment. For this purpose, a 100-Watt Sonopuls sounder (Bandelin) was used.
The fibres were manufactured in a laboratory spinner, whose structure enabled the stabilising of technological parameters at the levels desired, as well as their constant supervision and a broad-range of possibilities to change the process parameters. A spinneret with 500 orifices, each 0.08 mm in diameter, was used. The solidification of calcium alginate fibres was conducted in a bath containing 3% $CaCl_2$ and HCl. The drawing process consisted of two stages: The first drawing stage took place in a plastification bath containing 3% $CaCl_2$ and a small quantity of 0.03% solution of HCl. The second stage took place in saturated water vapour at a temperature of 135 ºC. Fibres were drawn in a continuous manner, by winding them on a reel. Following the drawing and rinsing, the fibres were dried in isometric conditions at a temperature of 25 °C.

Research methods

The rheological properties of the spinning solutions were determined using an Anton Paar rotational rheometer. The measurement was conducted at a shearing speed of 145 l/s and temperature of 20 °C with the use of an H-type cylinder. Rheological parameters *n* and *K* were determined on the basis of flow curves.

The tenacity of the fibres was determined in compliance with Standard PN-EN ISO 5079:1999.

The sorption was established in conditions of 65% and 100% relative humidity in compliance with Polish Standard PN-71/P-04653.

Water retention was determined with the use of a laboratory centrifuge, which enabled the mechanical disposal of water from the fibres during the centrifugation process at an acceleration of 10,000 m/s^2. The retention value was designated as the ratio of water mass remaining in the fibre after centrifugation to the mass of a totally dried fibre.

The porosity of the fibres was measured by means of mercury porosimetry using a Carlo-Erba porosimeter connected to a computer, enabling the estimation of the total volume and percentage of pores ranging between 5 - 7500 nm in size, as well as the total internal surface of the pores.

The distribution of the SiO_2 and Bioglass nanoadditives in the fibre was assessed on the basis of photographs taken with the use of scanning electron microscopy (SEM JSM 5400) equipped with an *EDX LINK ISIS* energy dispersion analyser for specific radiation (Oxford Instruments).

The degree of crystallinity and size of crystalline areas were determined by the wide-angle x-ray scattering (WAXS) method. The tests were performed using a URD 6 diffraction meter from Seifert (Germany) with a copper lamp emitting radiation of wavelength $\lambda = 1.54$ Å, with supply parameters U = 40 kV and I = 30 mA. The radiation used was monochromatised, with the help of a crystal monochromator. Diffraction curves were

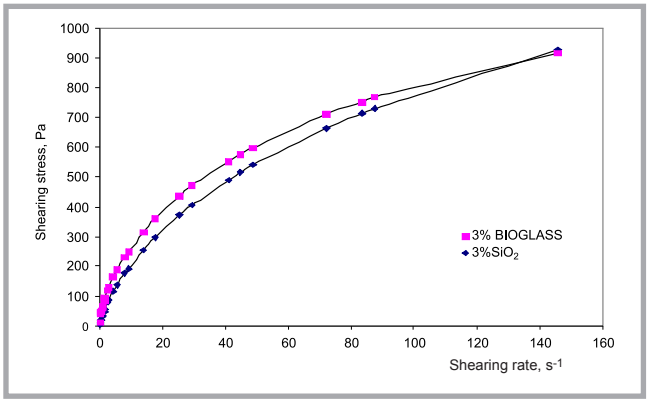

Figure 3. *Shearing stress as a function of the shearing rate for sodium alginate solutions LF 10/60/LS, concentration 7.4%, with 3% content of bioglass and SiO_2.*

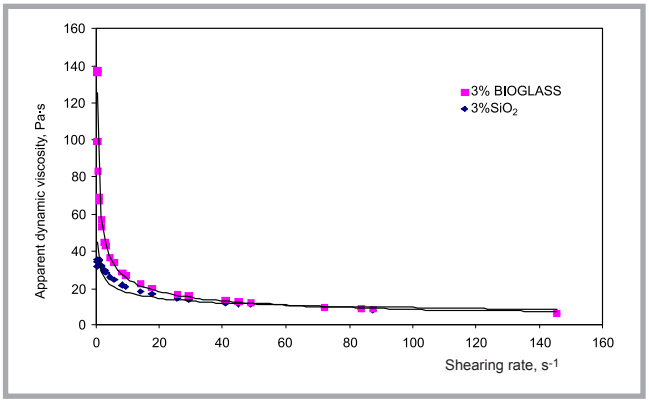

Figure 4. *Apparent dynamic viscosity as a function of the shearing rate for solutions of sodium alginate LF 10/60/LS, concentration 7.4%, with 3% content of bioglass and SiO_2.*

recorded using the reflection method and step measurement procedure. The fibres tested were powdered using a microtome to eliminate texture and then pressed into tablets of approximately 2 cm in diameter and 1 mm thickness. The detailed methodology for determining the degree of crystallinity and dimensions of crystallites is described in [19, 20].

Discussion of results

Analysis of the rheological properties of the spinning solutions

Knowledge of the rheological properties of spinning liquids plays an important role in assessing the stability of the forming process. The rheological nature of the liquid affects the distribution of speeds during the flow of liquid in the channel of the as-spun draw ratio, the stream widening effect outside the as-spun draw ratio, and changes the lengthwise speed gradient along the forming route. This value, which is connected with the force of collection of the fibres, determines the orientation of structural elements in the solidifying stream and the susceptibility of that structure to deformation processes at the drawing stage. In consequence, it affects the strength properties of the fibres.

According to our earlier findings [19, 20], the rheological properties of solutions of sodium alginate are affected by the presence in them of such nanoadditives as HAp, TCP and MMT. The structure of particular nanoadditives, their degree of fineness and tendency to agglomerate are dependent on interactions between the polymer macromolecules, solvent and nanoadditives. Analysis of the flow curves (***Figure 3***) shows that the introduction of sodium alginate with an SiO_2 or bioglass nanoadditive into the spinning solution (as in the case of other ceramic nanoadditives) does not alter the rheological character of the liquid: it is still a non-Newtonian fluid, diluted by shearing, without a flow boundary. The presence of nanoadditives does, however, affect the value of rheological parameters *n* and *k* in Ostwald de Waele's equation [19, 20] describing fluids of this type (***Table 1***).

Table 1. *Rheological parameters of a 7.4% solution of sodium alginate with SiO_2 and Bioglass.*

Sample symbol	Rheological parameters	
	n	k
7.4% Alg Na^+ + 3% SiO_2	0.675	36.02
7.4% Alg Na^+ + 3% Bioglass	0.549	68.30

The solution containing SiO_2 as a nanoadditive is closer to a Newtonian fluid. This also shows a less polymeric character than the solution containing bioglass. For this solution the value of rheological parameter *k* (being a measure of the consistency of the solution) is almost twice as large: k = 68.3. Corresponding to this are the curves shown in ***Figure 4***, representing the changes in apparent dynamic viscosity as a function of the shearing rate.

Based on a known explanation of the mechanism of dilution by shearing [21], the following interpretation can be given for the various rheological properties of the two solutions of sodium alginate tested. When shearing stresses are acting, macromolecules (which are tangled when in immobile liquid) become straightened out, between which are nanoadditives distributed in the continuous phase (solvent). As the shearing rate increases, the effect of straightening out is more and more marked. As a result, the internal friction of the system decreases due to a reduction in the effective dimensions of the macromolecules. The internal friction of such a system is affected by the dimensions of the nanoadditive particles. Furthermore, the effective dimensions of macromolecules with the nanoadditives located between them will be dependent on their dimensions. The high value of the consistency coefficient *k* of solutions with bioglass particles is explained by the average size of these particles, being around 100 – 200 nm. The diameters of bioglass particles are markedly greater than those of nanosilica (80 – 100 nm). The changes in the values of rheological parameters *n* and *k* considered are also consistent with the explanation of the mechanism of dilution by shearing associated with solvation [21]. As the shearing rate increases, the stripping of the solvation envelope becomes more effective. The effectiveness of this process also depends on the presence of nanoadditives in the system and the size of their particles.

Moreover, the effect of a reduction in the system's internal friction depends on the degree of differentiation of the sizes of nanoadditive particles occurring in the solution and on the nature of surface interactions between them, polymer macromolecules and the solvent.

Analysis of the porous structure and sorptive properties

Analysis of the sorptive properties of alginate fibres containing an SiO_2 or bioglass nanoadditive shows that an increased pull-out value at an as-spun draw ratio in an increasingly positive direction

Table 2. *Porous structure and sorptive properties of calcium alginate fibres with SiO_2 and Bioglass nanoadditive; *AS1 – AS5 – alginate fibres with SiO_2, AB1 – AB5 – alginate fibres with Bioglass.*

Sample symbol*	As-spun draw ratio, %	Total drawing, %	Content of Ca^{++}, %	Total volume of pores, cm^3/g	Volume of pores (3 - 1000nm), cm^3/g	Total internal surface of pores, m^2/g	Moisture sorption at 65% RH, %	Moisture sorption at 100% RH, %	Water retention, %
AS 1	+50	91.67	7.82	0.170	0.093	8.17	23.98	45.97	99.75
AS 2	+70	88.09	8.59	0.172	0.077	8.44	24.01	45.81	95.22
AS 3	+90	88.10	8.33	0.216	0.106	11.80	24.80	45.71	89.11
AS 4	+110	73.11	8.91	0.259	0.143	20.84	25.66	45.76	91.70
AS 5	+120	73.10	8.27	0.211	0.098	12.06	24.00	42.37	86.58
AB 1	+50	89.44	8.77	0.176	0.093	10.94	23.21	42.34	106.33
AB 2	+70	91.60	8.62	0.143	0.059	6.53	24.13	45.87	95.86
AB 3	+90	85.39	8.72	0.239	0.126	20.03	24.50	46.02	102.36
AB 4	+110	79.06	8.50	0.213	0.102	10.16	24.37	45.68	104.65
AB 5	+120	61.02	8.51	0.203	0.100	15.64	24.86	48.34	118.40

does not cause significant changes in these properties. This is true in spite of differences in the total volume of pores of the fibrous material investigated (***Table 2***). For fibres containing SiO_2 the total volume of pores is in the range 0.17 – 0.26 cm^3/g, and for fibres containing bioglass the range is 0.14 – 0.24 cm^3/g. At the same time the porosity of these fibres in a range up to 1000 nm (P_1) is low, between 0.06 and 0.14 cm^3/g. The total volume of pores of the fibrous material includes both the porosity of the fibres themselves (P_1) and that resulting from defects in the surface of the fibres and the space between monofilaments (P_2). Based on an analysis of cross-sections, lengthwise views and the work of Nagy et al. [22], it was concluded that the porosity of the fibres was due to pores with a radius in the range 3 – 1000 nm. However, the second range of porosity (P_2) includes pores between 1000 and 7500 nm. Comparison of the sorptive properties of the two types of nanocomposite fibres shows that, as for fibres containing other nanoadditives [19, 20], the sorption of moisture at 65% RH and 100% RH is determined by the hydrophilic nature of the material. The sorption of moisture at 65% RH for both types of fibres is between 23.2% and 25.6%. The sorption at 100% RH (depending on the pull-out at the as-spun draw ratio) is in the range 42 – 46% for fibres containing SiO_2, and 42 – 48% for fibres containing bioglass. The value of this indicator is also influenced by the volume of pores in a range up to 1000 nm and by the nature of the porous structure produced. However, in the case of hydrophilic material, this influence is limited. Not only do both types of fibres have a low level of porosity in a range up to 1000 nm, but also the nature of the porous structure in this range is subject to small changes, which is indicated by the nature of the curves representing the percentage distribution of pores by radius (***Figure 5***). The sorption of moisture at 100% RH is due to pores in the range 3 – 12.3 nm, which are capable of absorbing moisture through capillary condensation (this corresponds to the first maxima in ***Figure 5***).

However, the high maxima in the range of very large pores, with sizes of up to 7500 nm, relate to (as has already been mentioned) the empty spaces between fibres, or may also result from surface defects (***Figure 5***). Their contribution is nonetheless significant because these pores (also present in composite material) will favour the penetration of systemic fluids and the adhesion of newly formed cells. This type of porosity of fibrous material may also affect the water retention value. A result may be the linking of polymorphous clusters of water via hydrogen bridges with unsubstituted –OH groups of the fibre material. This will lead to the retention of water and, in particular, defects on the fibre surface. The water retention value for both fibres considered is dependent not only on the porous nature of their structure but also on the possibility of water penetration into amorphous areas of the material, which is accompanied by an increase in the lateral dimensions of the fibres (swelling), a known phenomenon for hydrophilic material. In the case of hydrophobic material, this phenomenon does not occur, and the water retention value is mainly accounted for by large pores in the range 75 – 750 nm [23]. The water retention value of fibres containing SiO_2, depend-

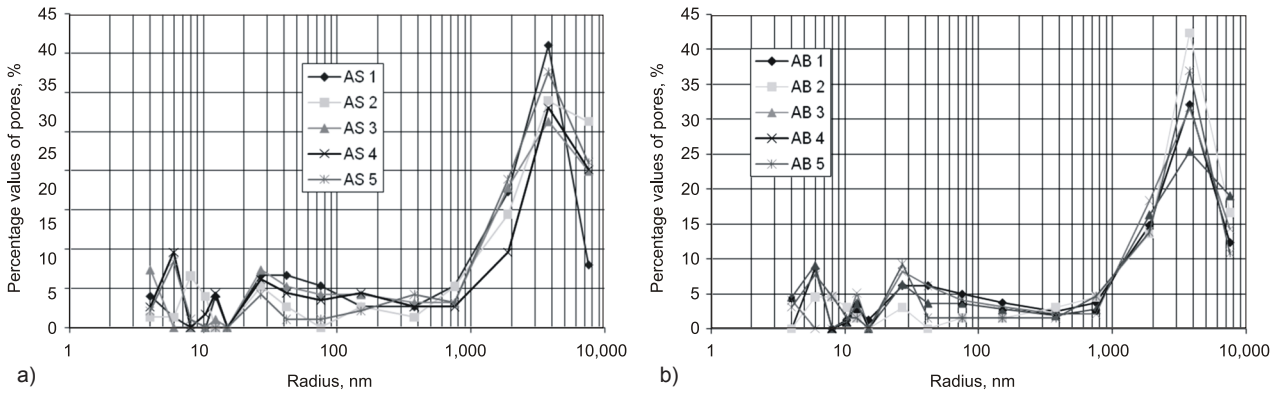

Figure 5. *Porous structure of calcium alginate fibres with; a) SiO_2, b) bioglass.*

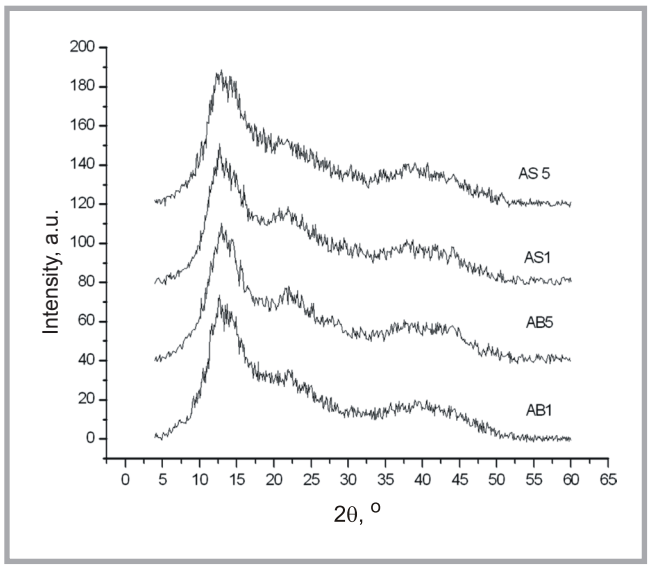

Figure 6. *WAXS diffraction curves for alginate fibres after elimination of the background and normalisation; AS1: fibers with the nanoadditive SiO_2 formed at an as spun draw ratio of +50%, AS5: fibers with the nanoadditive SiO_2 formed at an as spun draw ratio of +120%, AB1: fibers with the nanoadditive bioglass formed at an as spun draw ratio of +50%, AB5: fibers with the nanoadditive bioglass formed at an as spun draw ratio of +120%; The curves have been transposed vertically relative to each other for better visualisation.*

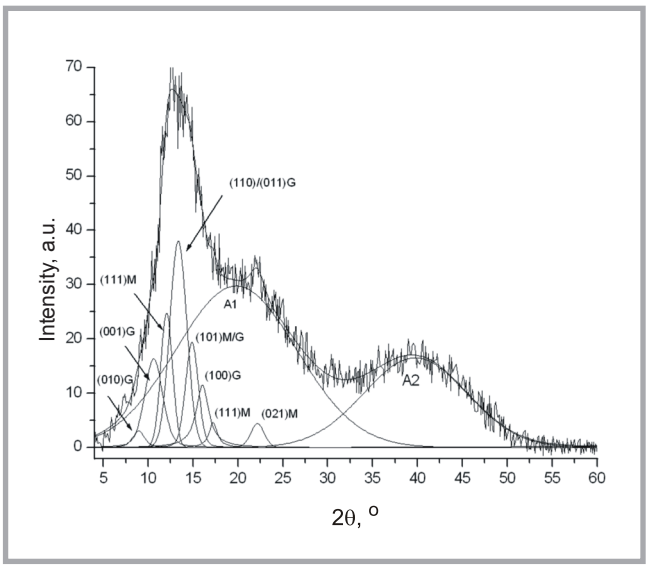

Figure 7. *Diffraction curve distribution for alginate fibres with the bioglass nanoadditive, formed at an asspun draw ratio of +50% – sample AB1. Miller indices are shown in the diagram for individual crystalline peaks. The peaks originating from crystallites built of mannuronic and guluronic blocks are labelled M and G, respectively. Amorphous components are labelled A1 and A2.*

a.u. - arbitrary units

ing on the pull-out applied at the as-spun draw ratio, is between 86% and 99%. Fibres containing bioglass have a higher water retention value, in the range 95 – 118%. Differences in the water retention values of the two types of fibres may also result from the different chemical structure of the nanoadditives and their tendency to agglomerate, which is greater in the case of the bioglass nanoadditive (***Figure 2***). In this situation the effect of the variable parameters of the forming process as well as of the pull-out at the as-spun draw ratio and total drawing on the water retention value for both types of fibres considered is difficult to specify.

Analysis of the supramolecular structure and strength properties

The strength properties of fibres are associated with both the axial orientation of macromolecules and their supramolecular structure.

Figure 6 shows normalised WAXS diffraction curves for fibres containing both types of nanoadditive, formed with the pull-out at the smallest (AB1 and AS1) and largest (AB5 and AS5) as-spun ratio values. All curves seem to be very similar, which means that the conditions of formation and the type of nanoadditive have little effect on the degree of crystallinity and on the quality of the crystalline structure of these fibres.

In the investigation of the degree of crystallinity and dimensions of crystallites using the WAXS method, the diffraction curves were distributed into crystalline peaks originating from crystalline areas built of guluronic and mannuronic blocks, and amorphous maxima. A detailed description of the calculation method is contained in [19]. An example diffraction curve distribution for sample AB1 is shown in ***Figure 7***. For all fibres tested, the values of the degree of crystallinity determined (***Table 3***) remain at a very similar and relatively low level: 24 – 27%. The differences which occur are of a random nature and are not associated with changes in the values for the pull-out at the as-spun draw ratio or total drawing.

The dimensions of crystallites determined on the basis of the widths of crystalline peaks deriving from different grid planes are in the range 3.5 – 6.8 nm (***Table 4*** see page 16). There is no clear correlation between the dimensions of the crystallites and the conditions of fibre formation. The differences occurring between the sizes of guluronic and mannuronic crystallites are below the margin of error of the measurement, which, due to the significant overlapping of peaks (see ***Figure 7***), is of the order of 1 nm.

Table 3. *Degree of crystallinity and size of crystallites in alginate fibers with Bioglass and silica nanoadditives; D_{100} (M) – average size of crystallites in the direction perpendicular to the planes (100) in crystallites formed of M blocks. $D_{110\,/\,011}$ (G) - average size of crystallites in the direction perpendicular to the planes (110) and (011) in crystallites formed of G blocks. D_{101} (M /G) - average size of crystallites in the direction perpendicular to the planes (101) both in crystallites formed of M and G blocks.*

Sample symbol	Degree of crystallinity, %	D_{100} (M), nm	$D_{110\,/\,011}$ (G), nm	D_{101} (M /G), nm
AB1	26 ± 0.78	5.7	4.0	5.3
AB2	26 ± 0.78	5.0	4.3	6.4
AB3	26 ± 0.78	4.7	4.2	5.8
AB4	25 ± 0.75	5.5	4.1	5.9
AB5	25 ± 0.75	5.3	4.4	6.0
AS1	24 ± 0.72	5.4	4.1	5.9
AS2	24 ± 0.72	5.3	4.2	5.2
AS3	27 ± 0.81	5.6	3.8	4.9
AS4	25 ± 0.75	5.4	4.1	6.8
AS5	27 ± 0.81	4.7	3.5	6.3

Table 4. *Strength properties of calcium alginate fibres with SiO_2 and Bioglass nanoadditives; σ_0 – stress in the solidification process, σ_1 – stress in the first drawing process (plastification bath), σ_2 – stress in the second drawing process (saturated water vapour at a temperature of 135 ºC).*

Sample symbol	As-spun draw ratio, %	Total drawing, %	Total deformation	Drawing stress, cN/tex			Tenacity, cN/tex	Elongation of break, %
				σ_0	σ_1	σ_2		
AS 1	50	91.67	2.875	0.032	1.257	1.152	21.98 ± 0.60	9.17 ± 0.53
AS 2	70	88.09	3.197	0.047	1.625	1.453	22.86 ± 0.69	9.23 ± 0.47
AS 3	90	88.10	3.574	0.047	2.270	2.242	21.35 ± 0.74	8.52 ± 0.47
AS 4	110	73.11	3.635	0.034	1.486	2.101	19.13 ± 0.94	8.35 ± 0.60
AS 5	120	73.10	3.808	0.066	2.045	2.249	19.10 ± 1.08	8.10 ± 0.77
AB 1	50	89.44	2.842	0.022	1.167	0.894	18.31 ± 0.89	7.72 ± 0.77
AB 2	70	91.60	3.253	0.030	1.664	1.475	19.53 ± 1.07	6.71 ± 0.80
AB 3	90	85.39	3.522	0.039	1.728	2.003	21.93 ± 0.87	6.96 ± 0.62
AB 4	110	79.06	3.756	0.043	2.160	2.149	24.73 ± 1.08	7.20 ± 0.65
AB 5	120	61.02	3.538	0.034	0.724	1.402	16.79 ± 0.79	6.97 ± 0.77

The low values of the degree of crystallinity of alginate fibres are caused by the high concentration of calcium ions in the fibres. These ions enable the formation of zones of 'egg-box' links between guluronic blocks located in neighbouring macromolecules of alginate [19]. Such links significantly restrict the freedom of movement of macromolecules and their ability to line up parallel to each other. Thus the ability of the fibre material to crystallise is significantly reduced, and hence the degree of crystallinity decreases. On the other hand, zones of egg-box links between molecules provide a very significant strengthening of the amorphous areas of the fibre, and as a result, in spite of the low degree of crystallinity, the tenacity of the fibres is relatively high.

The strength properties of the fibres are dependent on the value of the pull-out applied at the as-spun draw ratio and on the associated deformation at the drawing stage. Graphs of the changes in tenacity as a function of both of these process parameters show a clear maximum (***Figure 8***). However, the position of the maxima for fibres containing the two types of nanoadditive is different. In the case of fibres containing SiO_2, the highest tenacity (22.86 cN/tex) is achieved by fibres formed with a pull-out value at the as-spun draw ratio of +70%, which is similar to that of nanoadditives previously investigated [19, 20]. However, for fibres containing bioglass, the highest tenacity (24.73 cN/tex) is obtained when the forming process takes place with a pull-out value at the as-spun draw ratio of +110%. At the same time, the value of the degree of total draw obtainable is at a fairly low level - 79.06% in this case (***Table 4***). Nonetheless, deformation processes occur at all stages under the influence of the highest stresses in the series (***Table 4***). This is probably the reason why the highest tenacity is obtained for fibres formed at a pull-out of +110%.

In the case of fibres containing nanosilica, the high strength properties were due to both the high value of the total draw and the high value of stresses in all of the deformation processes (***Table 4***). However, the structure created at the solidification stage (when the pull-out applied at the as-spun draw ratio was +70%) was shaped by higher stresses than, for example, when the pull-out value was +50% (***Figure 9***). In spite of the lower susceptibility of the structure to deformation at the drawing stage, this produced the greatest tenacity in the whole series. However, the differences in the strength of fibres formed with a pull-out at an as-spun draw ratio ranging from +50 to +90% are not great. The same pattern has been found for alginate fibres containing other nanoadditives [19, 20]. Hence, these facts confirm that the strength properties of fibres are determined not only by the achievable value of the total stretch but also in equal measure by the value of stresses under which the structure is shaped at the solidification stage and reconstructed at subsequent stages of plasticisation drawing.

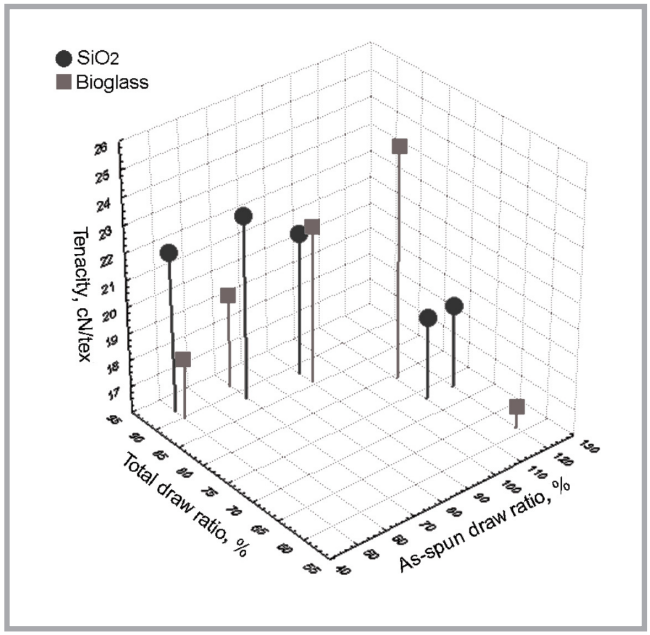

Figure 8. *Tenacity as a function of the as-spun draw ratio and total draw ratio for alginate fibres with the nanoadditives.*

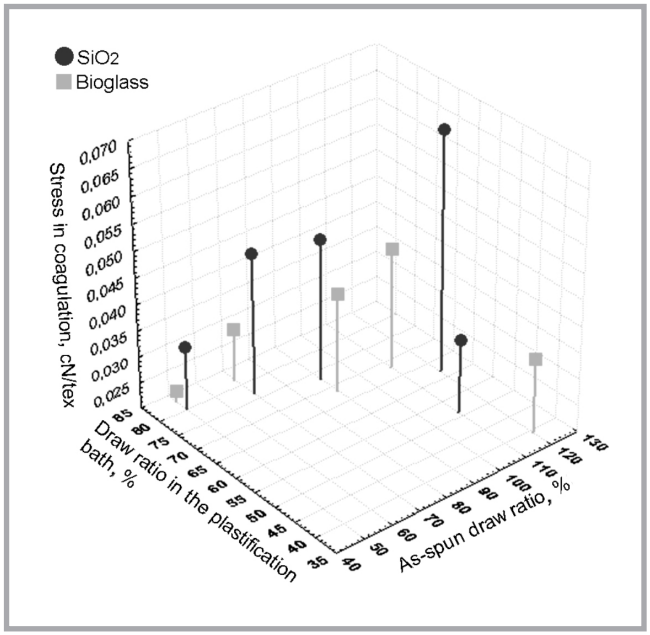

Figure 9. *Stress in coagulation (solidification) as a function of the as-spun draw ratio and draw ratio in a plastification bath for alginate fibres with the nanoadditives.*

Given the rigid structure of a macromolecule of the material, a significant role is played by the deformation of the still fluid stream and the orientation of structural elements in the direction of the fibre axis. This is dependent on the value of the pull-out at the as-spun draw ratio. The effect of the deformation of the still fluid stream is clear in the case of fibres containing bioglass. The highest values for the tenacity of these fibres is connected with the use of high positive (+110%) values for the pull-out at the as-spun draw ratio. The reasons for this can be found in the structure of the nanoadditive and its interactions with the polymer matrix. The strength of fibres formed with a +110% pull-out at the as-spun draw ratio is as much as 5.6 cN/tex greater than that of fibres containing the SiO_2 nanoadditive formed at an analogous as-spun draw ratio.

As has already been mentioned, fibre strength properties are subject to a very significant positive effect from the presence of zones of egg-box links between alginate macromolecules. For this reason, an important factor helping to determine the strength properties of fibres is the degree of substitution of sodium ions with calcium ions, because the calcium ion concentration determines the number of such zones. At similar degrees of the substitution of sodium ions with calcium ions, at a level of 7.8% – 8.9%, and degrees of crystallinity in the range of 24 to 27, the strength properties will also be dependent on the possibility of secondary links forming between macromolecules of the material. The presence of a nanoadditive, particularly in larger agglomerates, will make it harder for macromolecules to come close to each other. It will also affect the course of deformation processes.

Another factor is the type of nanoadditive introduced [19, 20]. According to the data given in ***Table 5***, the tenacity of calcium alginate fibres decreases in the following sequence:

$$\text{Alg(Ca)} \rightarrow \text{Alg(Ca+HAp)} \rightarrow \rightarrow \text{Alg(Ca+MMT)} \rightarrow \text{Alg(Ca+TCP)} \rightarrow \rightarrow \text{Alg(Ca+SiO}_2\text{)}$$

This table does not include fibres containing bioglass, because with these (as has already been analysed) the highest strength value is obtained when the forming process takes place with the pull-out at an as-spun draw ratio of +110%.

Table 5. *Tenacity of calcium alginate fibres with and without a nanoadditive.*

Type of fibres	As-spun draw ratio, %	Total drawing, %	Drawing stress, cN/tex			Tenacity, cN/tex
			σ_0	σ_1	σ_2	
AlgCa+HAp	+70	103.58	0.050	2.628	2.291	26.03 ± 0.97
AlgCa+TCP	+70	89.27	0.029	1.850	1.605	24.39 ± 0.71
AlgCa+MMT	+70	100.66	0.032	2.113	1.799	25.95 ± 0.80
AlgCa+SiO_2	+70	88.09	0,047	1,625	1,453	22.86 ± 0.69
AlgCa+bioszkło	+110	79.06	0,043	2,160	2,149	24.73 ± 1.08
AlgCa	+70	120.40	0.030	2.719	2.156	28.07 ± 0.68

Analysis of the data contained in ***Table 5*** shows that with the reduction in strength properties over the sequence as given, the reduction in the susceptibility to deformation at the drawing stage leads to a decrease in the strength properties of the fibres. With identical parameters of the solidification process and drawing stages, the highest value R_c = 120% is obtained for fibres without nanoadditives, and the lowest value R_c = 88.1% for fibres containing SiO_2. At the same time, the drawing process in a plasticisation bath takes place at this stage under the action of stresses which are lower by 1.1 cN/tex in comparison with fibres without a nanoadditive [19]. The result of this is a reduction in the tenacity of fibres containing SiO_2 by 5.2 cN/tex in comparison with fibres without a nanoadditive. It can therefore be assumed that the presence of ceramic nanoadditives in the solidifying stream and stretched fibre will affect the internal friction of the system being subjected to deformation processes. This friction will depend on the size of particles of the nanoadditive and its interactions with macromolecules

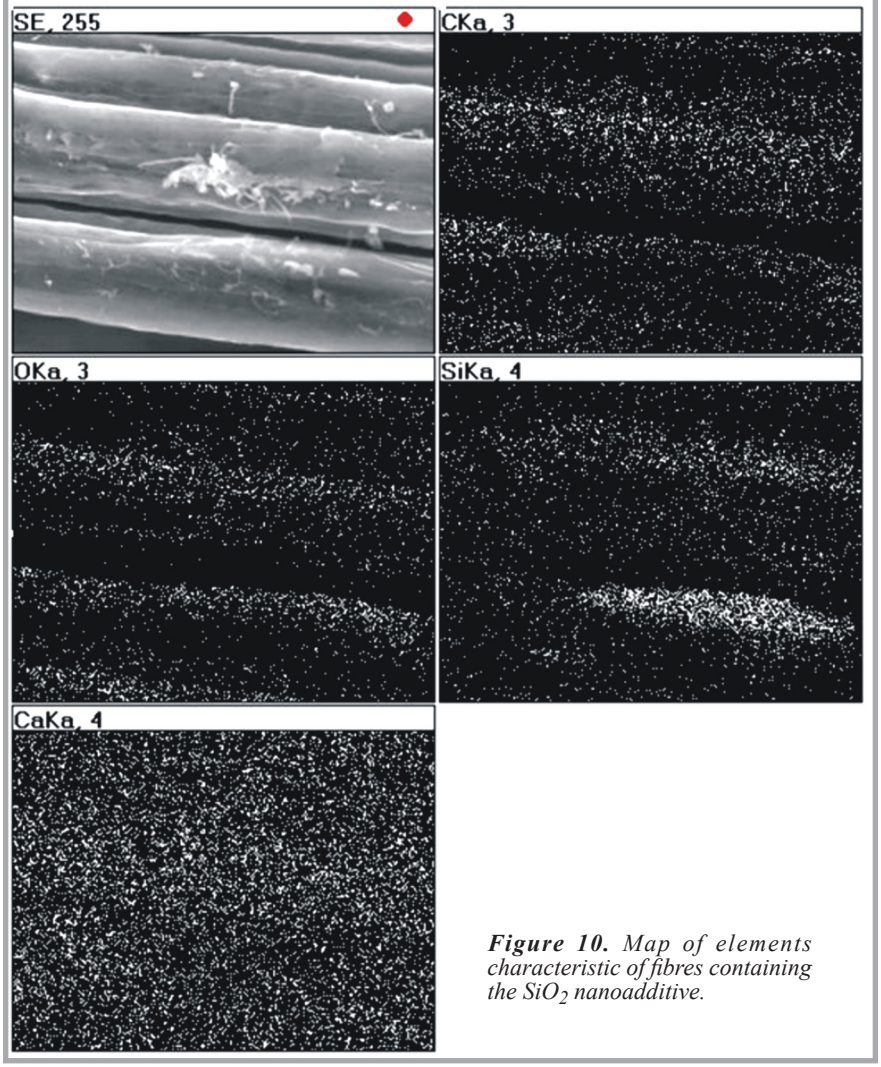

Figure 10. *Map of elements characteristic of fibres containing the SiO_2 nanoadditive.*

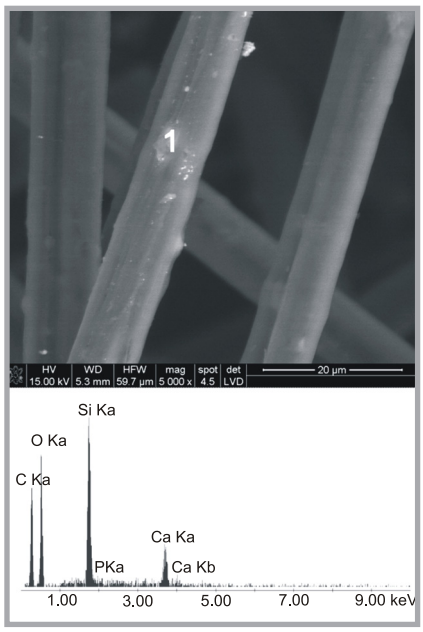

Figure 11. *SEM+EDS point analysis for fibres containing the bioglass nanoadditive.*

of the material. The presence of the nanoadditive between macromolecules will make it harder for them to slide relative to each other, which will cause a reduction in the deformation achievable. At the same time, the process takes place under the influence of lower stresses compared with fibres without a nanoadditive [19]. Both of these parameters affect (as has been analysed) the strength properties of the fibres. For fibres containing SiO_2 or bioglass nanoadditives, the relationship between the stress at the solidification stage, the pull-out at the as-spun draw ratio and the deformation achievable in the plasticisation bath is shown in ***Figure 9,*** see page 17. The nature of these dependencies for both types of fibres is consistent with the changes in their tenacity as a function of the pull-out at the as-spun draw ratio and total draw (***Figure 8,*** see page 17). It can therefore be concluded that there exists a certain optimum value of stress which favours production at the solidification stage of a structure susceptible to further reconstruction in subsequent deformation processes. When the stress values are too low, use is not made of the potential capabilities of the material. For fibres containing SiO_2, such a structure is created when the pull-out at the as-spun draw ratio is +70%. For fibres containing bioglass, the pull-out value is +110%. When these pull-out values are exceeded, the deformation achievable at the drawing stage is reduced. At the same time, the process takes place under the influence of decreasing stresses, which results in a reduction in the tenacity of both types of fibres. This value is lower than the maximum value by 3.76 cN/tex in the case of fibres containing SiO_2, and by as much as 7.94 cN/tex in the case of fibres containing bioglass.

Depending on the pull-out applied at the as-spun draw ratio, the value of elongation at rupture for alginate fibres containing nanosilica varies over the small range of 8.1 – 9.2%. However, for fibres containing bioglass the values are somewhat lower - 6.7 – 7.7%.

SEM+EDS analysis

In the course of the research, SEM+EDS tests were carried out to demonstrate the presence on the surface of alginate fibres of nanoadditives introduced into the material. Based on these tests, an attempt was made to assess the uniformity of the distribution of individual nanoadditives on the fibre surface. The map made of characteristic elements occurring in the sample tested (***Figure 10*** see page 17) shows the presence of Si^{4+} originating from the nanoadditive introduced (nanosilica in this case). It should also be noticed that, apart from a fairly uniform distribution of the nanoadditive on the surface of the fibres, the mapping shows that fragments with a greater density of silica occur, which may indicate the occurrence of the phenomenon of agglomeration. Similar behaviour was observed for fibres containing bioglass. The sporadic occurrence of agglomeration is also indicated by point analysis (***Figure 11***), which implies that the fibre tested contains agglomerates of the nanoadditives.

Conclusions

The research performed enabled the determination of the influence of the basic parameters of the forming process on the structure and properties of nanocomposite alginate fibres, which was the basis for determination of the best fibre forming conditions, due to the values of their tenacity, for two types of calcium alginate nanocomposite fibres.

The high sorptive properties and water retention in calcium alginate fibres containing SiO_2 or bioglass nanoadditives are mainly due to the hydrophilic nature of the material. The possibilities of modifying these properties through appropriate selection of conditions for the formation of fibres are limited.

The strength properties of nanocomposite alginate fibres are determined not only by the value of the total stretch but also by the values of stresses under which the deformation processes take place at successive stages of fibre production.

A strength of over 22.5 cN/tex obtained for both types of fibres requires that the process of their formation be carried out at positive values for the pull-out at the as-spun draw ratio. This value is +70% for fibres containing nanosilica and +110% for those containing bioglass.

Acknowledgment

The research was financed by the Minister of Science and Higher Education in 2008-2010 as project No. 3809/B/T02/2008/35

References

1. *Hench L. L., Jones J. R.; Biomaterials, artificial organs and tissue engineering. Woodhead Publishing Limited: Cambridge, 2005.*
2. *Aebicher P., Schluep M., Deglon N., Joseph J. M., Hirt L., Heyd B., Goddard M., Hammang J. P., Zurn A. D., Kato A. C., Regli F., Baetge E. E.; Intrathecal delivery of CNTF using encapsulated genetically modified xenogeneic cells in amyotrophic lateral sclerosis patients, Nat. Med. 2, 1996, pp. 696-699.*
3. *Sheridan R. L., Tompkins R. G., Burke J. F.; Management of burn wounds with prompt excision and immediate closure, J. Intensive Care Med. 9, 1994, pp. 6-17.*
4. *Chen S. C., Mullon C., Kahaku E., Watanabe F., Hewitt W., Eguchi S., Middleton Y., Arkadopoulos N., Rozga J., Solomon B., Demetriou A. A.; Treatment of severe liver failure with a bioartificial liver, Ann. N. Y. Acad. Sci. 831, 1997, pp. 350-360.*
5. *Kin T., Iwata H., Aomatsu Y., Ohyama T., Kanehiro H., Hisanaga M., Nakajima Y.; Xenotransplantation of pig islets in diabetic dogs with use of a microcapsule composed of agarose and polystyrene sulfonic acid mixed gel, Pancreas 25, 2002, pp. 94-100.*
6. *Kadiyala S., Jaiswal N., Bruder S. P.; Culture expanded, bone marrow derived mesenchymal stem cells can regenerate a critical-sized segmental bone defect, Tissue Eng. 3, 1997, pp. 173-185*
7. *Naumann A., Rotter N., Bujia J., Aigner J.; Tissue engineering of autologous cartilage transplants for rhinology, Am. J. Rhinol. 12, 1998, pp. 59-63.*
8. *http://www.apligraf.com (07.12.2009).*
9. *http://www.dermagraft.com (07.12.2009).*
10. *http://www.biotissue.de/en-ProductsPatientsBioSeedCIntroduction.html (07.12.2009).*

11. *Stodolak E.; Badania nad modyfikacją powierzchniową i wpływem włókien na materiał polimerowy i odpowiedź komórkową, Praca doktorska AGH Kraków, 2006*
12. *Peltola T., Jokinen M., Veittola S., Rahiala H., Yli-Urpo A.; Influence of sol and stage of spinnability on in vitro bioactivity and dissolution of sol-gel derived SiO2 fibers. Biomaterials 22(6), 2001, pp. 589-598.*
13. *Hench L. L.; Bioceramics: From Concept to Clinic. J Am Ceram Soc 74(7), 1991, pp. 1487-1510.*
14. *Hench L. L.; Bioceramics. J Am Ceram Soc 81(7), 1998, pp. 1705-1728.*
15. *Yilmaz S., Efouglu E., Kilic A. R.; Alveolar ridge reconstruction and/or preservation using root form bioglass cones. J Clin Periodontol 25(10), 1998, pp. 832-839.*
16. *Tilocca A.; Short-and medium-range structure of multicomponent bioactive glasses and melts: An assessment of the performances of shell-model and rigid-ion potentials. J Chem Phys 129(8), 2008, pp. 484-504.*
17. *Yukna R. A., Evans G. H., Aichelman-Reidy H. B., Meyer E. T.; Clinical Comparison of Bioactive Glass Bone Replacement Graft Material and Expanded Polytetrafluoroethylene Barrier Membrane in Treating Human Mandibular Molar Class II Furcation. J Periodontol 72(2), 2001, pp. 125-133.*
18. *Zamet J. S., Darbar U. R., Griffits G. S., Bulman J. S., Brägger U., Bürgin W., Newman H. N.; Particulate bioglass® as a grafting material in the treatment of periodontal intrabony defects. J Clin Periodontol 24(6), 1997, pp. 410-418.*
19. *Boguń M., Mikołajczyk T., Rabiej S.; Effect of Formation Conditions on the Structure and Properties of Nanocomposite Alginate Fibres. J Appl Polym Sci 114, 2009, pp. 70-82.*
20. *Boguń M., Rabiej S.; The influence of fibre formation conditions on the structure and properties of nanocomposite alginate fibres containing tricalcium phosphate or montmorillonite. J Polym Composites -Published Online: Oct 1 2009, DOI: 10.1002/pc.20917.*
21. *Ferguson J., Kembłowski Z., Reologia stosowana płynów, Wydawnictwo Marcus sc, Łódź, 1995.*
22. *Nagy V., Laszlo M., Vas M.; Pore Characteristic Determination with Mercury Porosimetry in Polyester Staple Yarns. Fibres Text East Eur 13(3), 2005, pp. 21-26.*
23. *Mikołajczyk T., Modification of the Manufacturing Process of Polyacrylonitrile Fibres, Scientific Buletin of Technical University of Lodz, No 781, Scientific Theses Z 243, Lodz, 1997.*

Received 06.11.2009 Reviewed 25.01.2010